

RECEIVED  
MAILED  
NOV 9 1938

Library, L. M. a. L.

TECHNICAL NOTES

NATIONAL ADVISORY COMMITTEE FOR AERONAUTICS

No. 673

THE PRESSURE AVAILABLE FOR GROUND COOLING IN FRONT  
OF THE COWLING OF AIR-COOLED AIRPLANE ENGINES

By George W. Stickle and Upshur T. Joyner  
Langley Memorial Aeronautical Laboratory

Washington  
November 1938



3 1176 01425 6813

NATIONAL ADVISORY COMMITTEE FOR AERONAUTICS

TECHNICAL NOTE NO. 673

THE PRESSURE AVAILABLE FOR GROUND COOLING IN FRONT  
OF THE COWLING OF AIR-COOLED AIRPLANE ENGINES

By George W. Stickle and Upshur T. Joyner

SUMMARY

A study was made of the factors affecting the pressure available for ground cooling in front of a cowl. Most of the results presented were obtained with a set-up that was about one-third full scale. A number of isolated tests on four full-scale airplanes were made to determine the general applicability of the model results. The full-scale tests indicated that the model results may be applied qualitatively to full-scale design and quantitatively as a first approximation of the front pressure available for ground cooling.

INTRODUCTION

The problem of cooling an airplane engine on the ground consists in providing a pressure drop across the baffles to cool the rear of the cylinder and sufficient movement of the air in front of the engine to cool the front of the cylinder. The pressure drop across the baffles is the difference between the pressures in front of and behind the engine. The rear pressure depends on the design of the exit slot, which for ground operation is similar to that for flight conditions and is given in references 1 and 2. The conditions affecting the pressure in the front of the cowl for ground operation are entirely different from those in flight because, on the ground, the propeller effect is all important and, in flight, the main effect is that of the forward velocity of the airplane. The purpose of the work reported herein was to study the best methods of utilizing the propeller to produce pressure in front of the cowl. The main part of the investigation was conducted on a model set-up that was about one-third full scale.

After the model tests were completed, their general applicability was determined by extending the ground-cooling tests to include measurements on four full-scale airplanes.

### APPARATUS AND METHODS

In the model-test set-up, a 25-horsepower electric motor was used to drive the propellers. Cowlings were mounted on the motor in proper relation to the propeller location so that similarity to full-scale airplanes was obtained. The set-up is shown in figure 1. The seven cowlings, the various disks, the spinner, and the deflector are shown in figure 2. Two adjustable-pitch propellers were used; a 2-blade 48-inch-diameter propeller, designated propeller B (fig. 3); and a 3-blade 39-inch-diameter propeller, designated propeller C (fig. 1). It should be noted that propeller C has round-blade shanks corresponding to present-day practice and that propeller B has good airfoil sections near the propeller hub.

The general arrangement of the set-up can be seen in figure 1. The cowlings and disks were attached to the mounting tube shown enclosing the propeller shaft. The baffle plate was made by punching 1-inch holes in a sheet-metal disk. The conductivity of the baffle plate, corresponding to the combined engine and cowlings conductivity, was varied by the use of corks in these holes. The 12 $\frac{1}{2}$ -inch round-edge disk is shown in place in front of nose 2. The minimum free area between the cowlings and the disk is referred to as "the area of the front opening." The reference area  $F$ , defined as the maximum cross-sectional area of the cowlings, has a value based on a diameter of 20 inches for the model tests. The other disks and noses were mounted in the same manner as in the set-up shown in figure 1.

A study of the flow conditions in the front of the cowlings was made by the use of measurements of pressure distribution, observations of smoke flow, and measurements of air flow with a hot-wire anemometer. The pressure orifices were located in the baffle plate along the radius of the cowlings. The observations of smoke flow were made by introducing smoke in front of the propeller and observing the flow lines and also by introducing smoke between the baffle plate and the propeller and noting its behavior

inside the cowling nose. Since the front of the engine cylinder is cooled by the movement of air inside the front of the cowling, any device that changes the movement of air may affect the amount of cooling available. The relative cooling of the front of the cylinder with various combinations of cowlings and disks was determined by measuring the heat dissipated from a hot wire located in front of the baffle plate. The hot wire was maintained at constant temperature.

The full-scale airplanes used to determine the general applicability of the model test were modern airplanes with conventional baffling and cowlings. Several propellers were used on some of the airplanes to determine the effect of good and bad blade sections near the propeller hub. The pressure in front of and behind the baffles for several propeller speeds was measured.

The results are presented in the form of coefficients that are, in effect, nondimensional. The pressures  $p_f$ ,  $p_r$ , and  $\Delta p$ , which refer to the pressures in front of the baffles and behind the baffles and the pressure drop across the baffles, respectively, are divided by  $n^2 D^2$  to make the coefficients independent of propeller speed and scale, where  $n$  is the number of revolutions per second of the propeller and  $D$  is the propeller diameter in feet. In order to make these coefficients strictly nondimensional, they should be divided by the mass density of the air but, for all practical purposes, the density may be assumed constant and left out of the coefficients. A point along a radius of the cowling is located by using the quantity  $x = d/D$ , where  $d$  is twice the distance from the point to the propeller axis. The radial pressure distribution within a given cowling is presented as a plot of the pressure coefficient,  $p_f/n^2 D^2$ , against  $x$ . When the average pressure in front of the baffle plate is given as a function of the diameter of the front opening, the results are given as a plot of the integrated average pressure coefficient against  $x_1 = d_1/D$ , where  $d_1$  is the maximum diameter of the front opening.

Each arrangement of the model set-up was tested for several engine conductivities. When the conductivity  $K$  of the baffle plate is other than zero, that is, when air is flowing through the cowling, the area of the front opening becomes a restriction to the flow and consequently lessens the pressure at the front of the baffle. In order

to study effects of other variations of cowlings arrangements and to eliminate the effect of air flow, the condition for zero engine or baffle conductivity was used in describing the main part of the model-test results. The results for conductivity other than zero were used only to describe the effect of the area of the front opening.

## RESULTS AND DISCUSSION

The first consideration in regard to front pressure is the manner in which the available pressure varies with the propeller radius. In order to study this effect, nose 1 (fig. 2) was used and the pressure in each ring was determined. Noses 3 and 7 were used with circular disks to extend the investigation to larger radii than those obtainable with nose 1. The results of these tests are given for propeller B in figure 4(a) and for propeller C in figure 4(b). The pressure coefficient reaches a maximum for the 2-blade propeller B at a smaller radius than for the 3-blade propeller C, and the values for the 3-blade propeller reach a much higher value because of the increase in the propeller solidity. These plots picture the advantage to be gained by increasing the diameter of the nose opening and also suggest the possibility of blocking off the low-pressure area in order to obtain a uniform and a high pressure over the entire front of the engine. The effect of propeller blade-angle setting on the pressure coefficient is also given in figure 4. As would be expected, the blade angle setting has little effect close to the propeller hub but the effect increases as the radius increases.

The smoke-flow studies showed that a very peculiar condition existed with propeller B set  $10^\circ$  at  $0.75R$  in front of nose 2 for zero conductivity. The flow alternated between a rotating flow and a pulsating flow, or one in which the rotation stopped and the only motion was that of a very turbulent movement of the air in and out of the cowlings nose. The period of the changes from rotating to pulsating flow was very irregular but was of the order of 3 seconds. At times, the smoke introduced between the propeller and the baffle plate would shoot straight forward through the propeller disk to a distance almost equal to the propeller radius. Figure 5 shows the pressure distribution across the front for these two conditions of flow. With the rotating flow, the pressure available for cooling

was lessened at all radii and was zero at  $x = 0.16$ . With pulsating flow, the pressure was constant over the front and was very much higher, showing the desirability of the pulsating flow. When the conductivity of this set-up was increased, the instability in the flow disappeared and rotating flow was always present. If a single plate was placed perpendicular to the rotation between the baffle plate and the nose of the cowl, however, the flow could again be changed to the pulsating type, resulting generally in higher pressures but very poor circumferential distribution of pressure. With propeller C, the flow inside the front of the cowl always had a high circumferential velocity in the direction of the propeller rotation. Figure 6 shows the radial pressure distribution in three open-nose cowlings with propeller C. A comparison of the pressure distribution with that given in figure 5 shows that rotating flow is present for all three nose shapes and that the highest circumferential velocity is present for nose 7.

Two types of deflectors, a spinner, and several disks were tested to determine the best method of obtaining this high uniform pressure over the entire front of the engine. The results of the tests are given in figure 7, in which the average pressure coefficient over the front of the engine is plotted against the value of  $x_1$  for the front opening of the particular cowl. Each test gave one point in this figure. It is seen that, for small front openings, the deflectors seem to have some advantage over the flat disk but, for larger openings, the flat disk seems to be at least as good as any deflectors tried. Disks were therefore used as a means of maintaining high static pressure in front of the engine for the rest of the tests.

Since the propeller is acting as a low-pressure blower, the distance of the cowl from the trailing edge of the propeller is important as a leakage area; its effect on the pressure available is shown in figure 8. It is seen that the shortest distance between the propeller and the cowl is the best. It should be noticed in figure 8 that these distances are given in inches and apply to the model set-up and must be increased in the same ratio as the propeller diameter for application to the full-scale set-up.

Figure 9 shows the effect of the location of the disk within the nose of the cowling. In figure 9(a), which is for  $\frac{1}{2}$ -inch clearance between cowling and propeller, the best location of the flat disk is even with the front lip of the cowling. If the disk is moved forward, it deflects the flow and decreases the pressure; and, if it is moved backward, the circumferential flow has a greater opportunity to build up in front of the disk and thus decrease the pressure inside the cowling. The round-edge disk with the front part of the disk even with the nose is the best for the  $\frac{1}{2}$ -inch clearance between the cowling and the propeller. Figure 9(b) shows the same effect for the flat disk with a 2-inch clearance between the cowling and propeller. Again the position even with the cowling nose is the best. Figure 9(c) shows the 2-inch cowling clearance for the round-edge disk. These tests indicate that the face of the round-edge disk may be located farther forward than that of the flat disk without any detrimental effect, and a comparison of figure 9(c) with figure 9(b) shows that the round-edge disk is slightly better than the flat disk.

Figure 10 shows the effect of disk diameter for noses 2, 3, and 7. As would be expected, the larger the disk, the higher is the available pressure because the radius of the effective opening is increasing, giving an effect similar to that in figures 4(a) and 4(b). It can be seen from figure 10 that, with the largest disk, the radial pressure distribution over the front of the engine is similar to the pressure distribution for pulsating flow, as shown in figure 5, and that it gradually changes to the type for rotating flow as the size of the disk is reduced.

Figure 11(a) shows the average front pressure as a function of the ratio of the area of the front opening,  $A$ , to the area of the cowling cross section  $F$  for nose 2 with propeller  $\phi$  set  $15^\circ$  at  $0.75R$ . The zero conductivity shows that the smallest front area or the largest ( $17\frac{1}{2}$ -inch) disk is the best; with 0.061 total conductivity, the  $17\frac{1}{2}$ -inch disk restricted the flow too much and lowered the available pressure. With a total conductivity of 0.111, the  $17\frac{1}{2}$ -inch and the  $12\frac{1}{2}$ -inch disks restricted the flow more than the increase due to the change in radius and the  $10\frac{1}{2}$ -inch disk was the best. It should be noted that the round-edge disk gives a larger effective area than the flat-edge disk of the same dimensions. This result indicates that a round-edge disk is best because it allows smaller openings for the same front pressure loss and

gives a higher available pressure drop for cooling. This fact should be especially true with large conductivity when a large front opening will be required.

Measurements of the cooling properties obtained with hot-wire anemometers indicate that the cooling on the front of the barrel would be less with a disk in place but that the head cooling would be somewhat improved owing to the directed stream of air from the front opening. This result indicates that the improved pressure obtainable on the ground with the disk will be realized as improved cooling on both the front and the back of the cylinder heads and will give a large increase in cooling on the back of the barrel with some decrease in cooling on the front of the barrel.

Flight tests on a full-scale airplane showed that the cooling of the front of the cylinders was unchanged by the addition of a disk, which shows that the advantage of the disk on the ground will not be offset by bad effects in flight.

#### GROUND TESTS ON FULL-SCALE AIRPLANES

The ground tests on four full-scale airplanes represent isolated points of engine conductivity, front opening, propeller blade-angle setting and diameter, and one case of the use of a flat disk in front of the cowl. The results of these tests are given in table I and show substantial agreement with the model results. The increase of average front-pressure coefficient due to the addition of the flat disk shows about the same order of net increase as obtained on the model. The wide variation of the pressure drop available, from a coefficient of 0.061 on airplane 2 with a service propeller to 0.249 on airplane 1 with propeller B, is noteworthy.

#### CONCLUDING REMARKS

1. The available pressure in front of the cowl increased rapidly with propeller radius up to 30 or 40 percent of the propeller radius. The cowl should be located as close to the propeller as practicable.



2. Disks located in front of the nose of the cowling greatly increased the average pressure in front of the engine baffles. It is important that the plane of the disk be even with the nose of the cowling. A round-edge disk was superior to a straight flat disk. The size of the disk should be such that the area of the front opening is optimum for the total conductivity used.

3. Tests on full-scale airplanes showed that the model tests may be qualitatively applied to full-scale design and quantitatively applied as a first approximation of the available front pressure.

Langley Memorial Aeronautical Laboratory,  
National Advisory Committee for Aeronautics,  
Langley Field, Va., October 4, 1938.

#### REFERENCES

1. Theodorsen, Theodore, Brevoort, M. J., and Stickle, George W.: Full-Scale Tests of N.A.C.A. Cowlings. T.R. No. 592, N.A.C.A., 1937.
2. Theodorsen, Theodore, Brevoort, M. J., and Stickle, George W.: Cooling of Airplane Engines at Low Air Speeds. T.R. No. 593, N.A.C.A., 1937.

TABLE I. Results of Ground Tests on Full-Scale Airplanes

Air-plane	Propeller	Blade angle setting (deg.)	Number of blades	Propeller diameter (ft.)	Type of propeller	x for cowl-ing diameter	x <sub>1</sub> for front opening	A/F	Approximate conductivity of engine	$\frac{P_f \times 10^3}{n^2 D^2}$	$\frac{P_r \times 10^3}{n^2 D^2}$	$\frac{\Delta p \times 10^3}{n^2 D^2}$	Remarks
1	B	15	3	10	G	0.430	0.325	0.57	0.07	0.270	0.021	0.249	Flaps open
1	S	17	2	9	R	.478	.360	.57	.07	.208	.033	.175	Flaps open
2	B	15	3	10	G	.392	.270	.47	.06	.264	.124	.140	
2	S	13	2	9	R	.436	.300	.47	.06	.138	.077	.061	
2	S	18	2	9	R	.436	.300	.47	.06	.119	.051	.068	
3	B	15	3	10	G	.44	.325	.55	.15	.160	.040	.120	
3	C	26.1	3	10	R	.44	.325	.55	.15	.064	-.007	.071	
3	S	23.6	2	9.5	R	.46	.340	.55	.15	.093	.023	.070	
3	S	30.6	2	9.5	R	.46	.340	.55	.15	.130	.043	.087	
4	S	13	3	9-1/6	R	.508	.370	.53	.08	.241	.096	.145	
4	S	13	3	9-1/6	R	.508	.370	.53	.08	.290	.106	.184	With flat disk

The propellers and types of propellers are designated as follows:

S, service propeller.

B and C, propeller similar to the B and C propellers tested on the model set-up.

G, good blade sections near the hub.

R, round propeller-blade shanks.

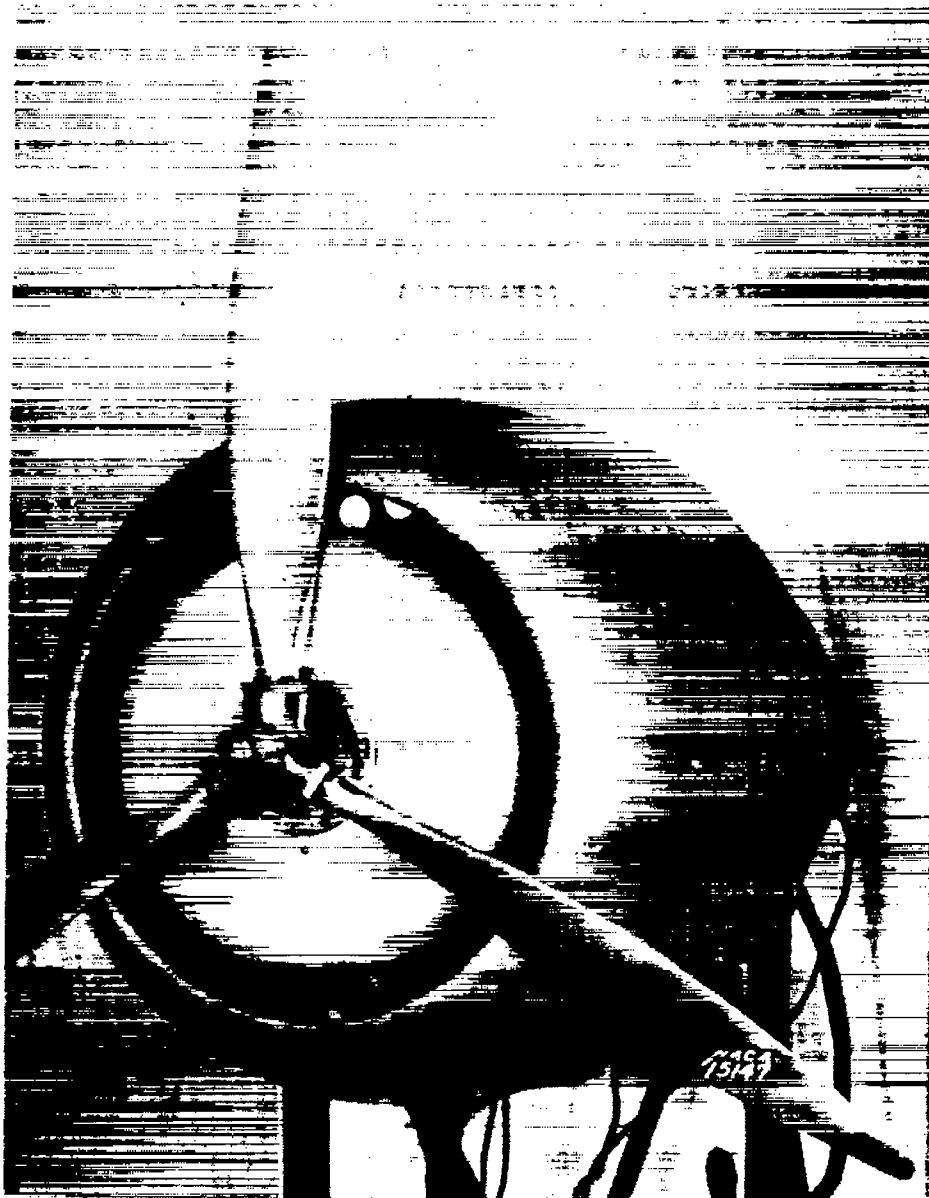


Figure 1.- Model set-up with nose 2 and propeller C  
with 12-1/2 inch round edge disk.



Figure 3.- Propeller B.

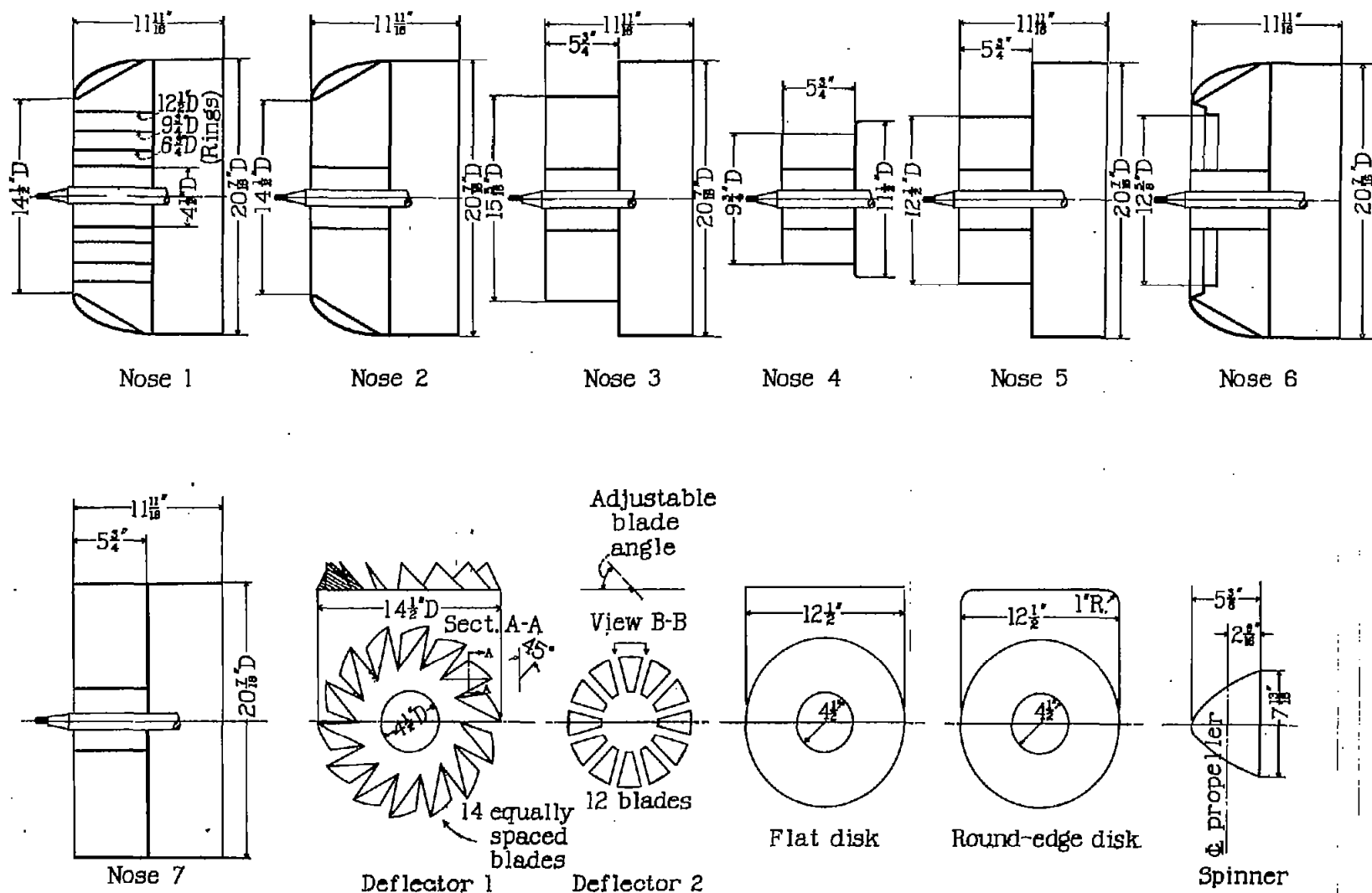


Figure 2.- Layout of nose shapes, spinner, disks, and deflectors used for the model tests.

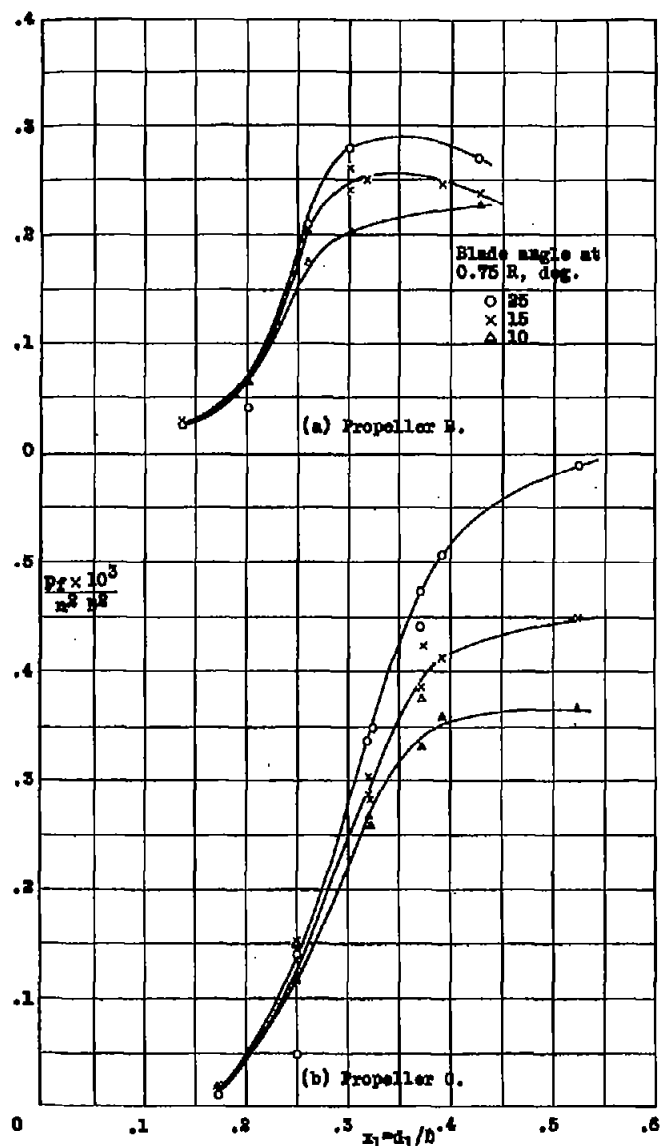


Figure 4.- Effect of propeller radius and blade-angle setting on the available front pressure.  $K = 0$ .

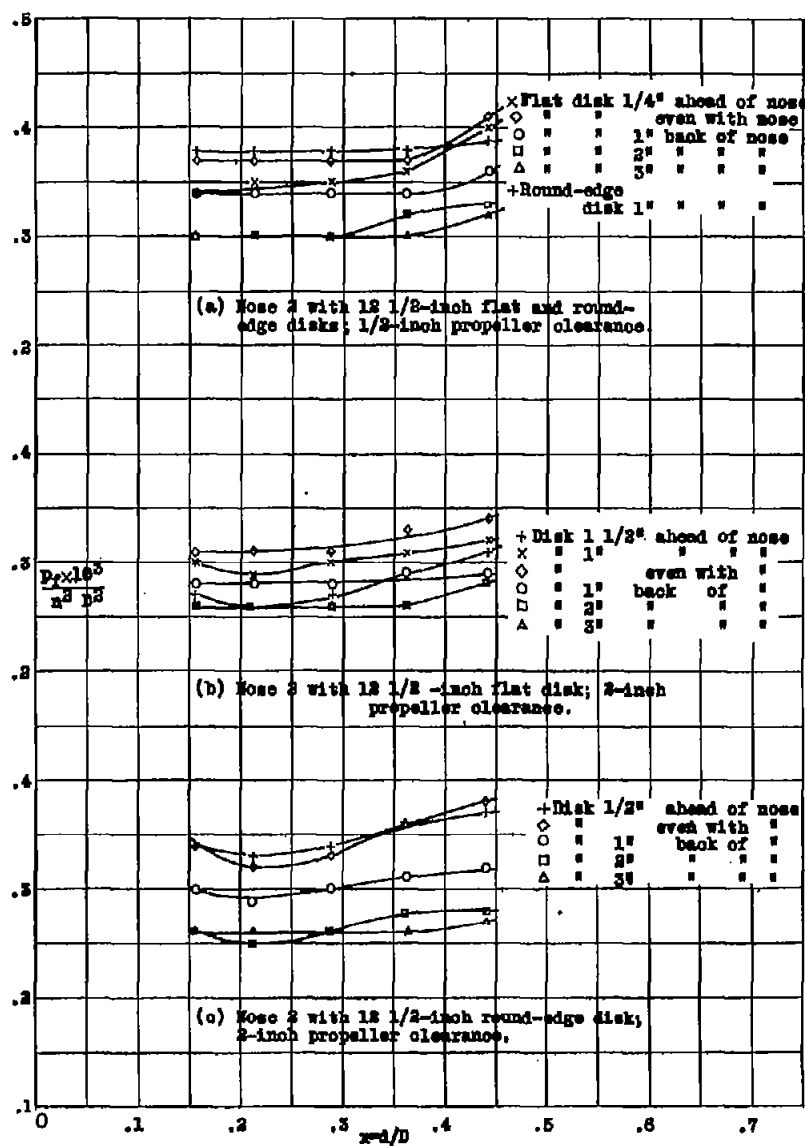


Figure 9.- Effect on the radial pressure distribution of the forward and backward location of the disk inside the nose of the cowling. Propeller C set .15 at  $0.75 R$ ;  $K = 0$ .

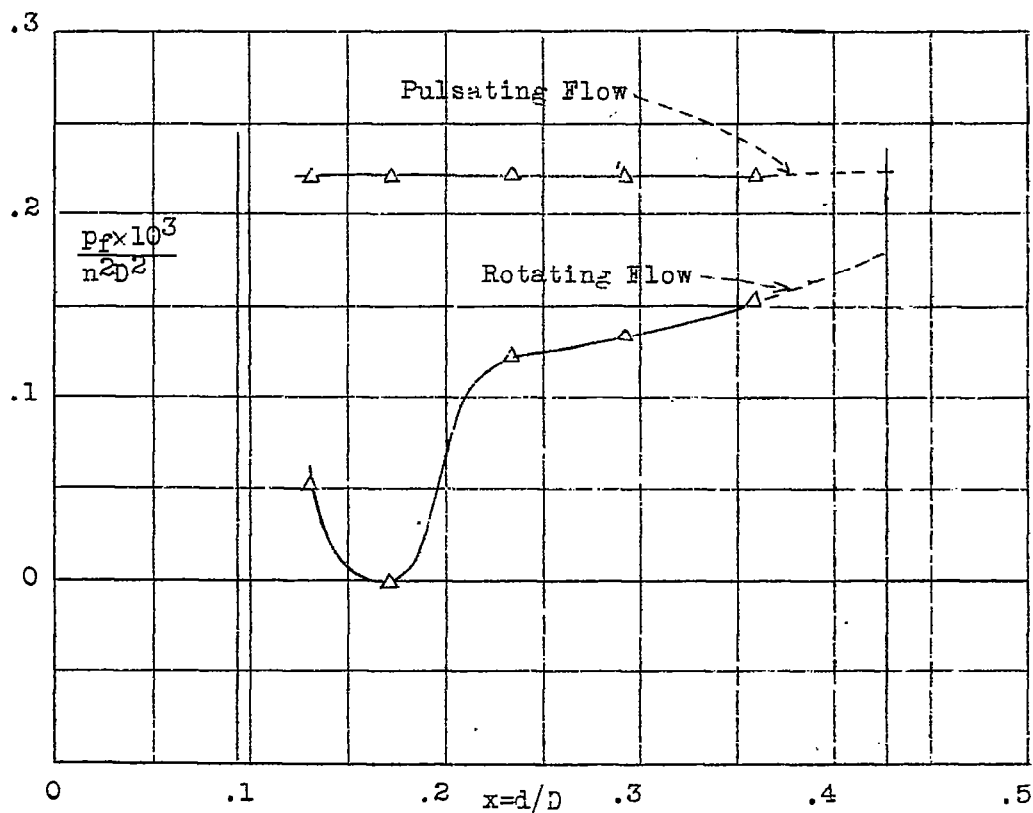


Figure 5.- Effect of flow conditions on the radial pressure distribution inside the nose of the cowling. Nose 2; propeller B; blade angle  $10^\circ$  at  $0.15 R$ ,  $K=0$ .

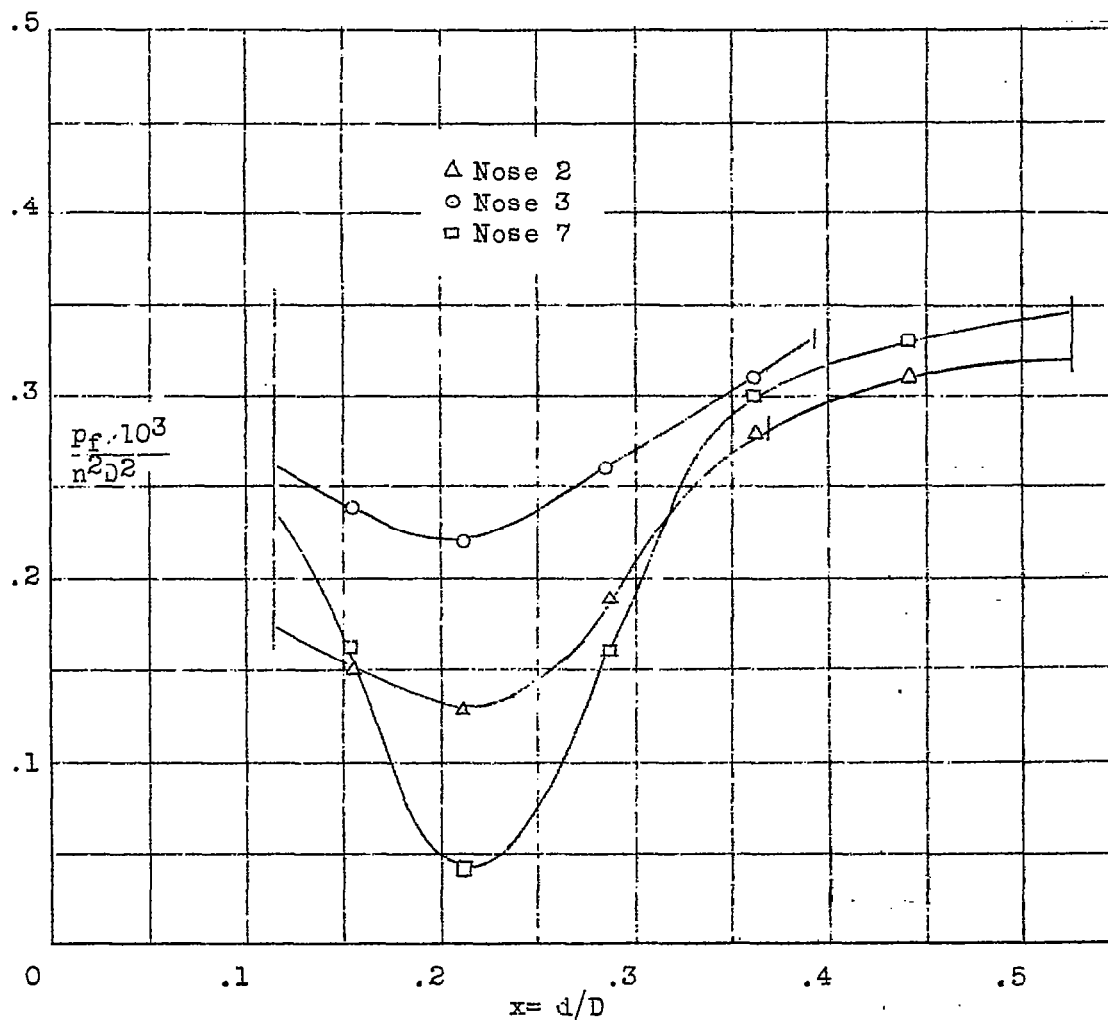


Figure 6.- Effect of flow conditions on the radial pressure distribution inside the nose of the cowl. Propeller C; blade angle  $15^\circ$  at  $0.75 R$ ,  $K=0$ .

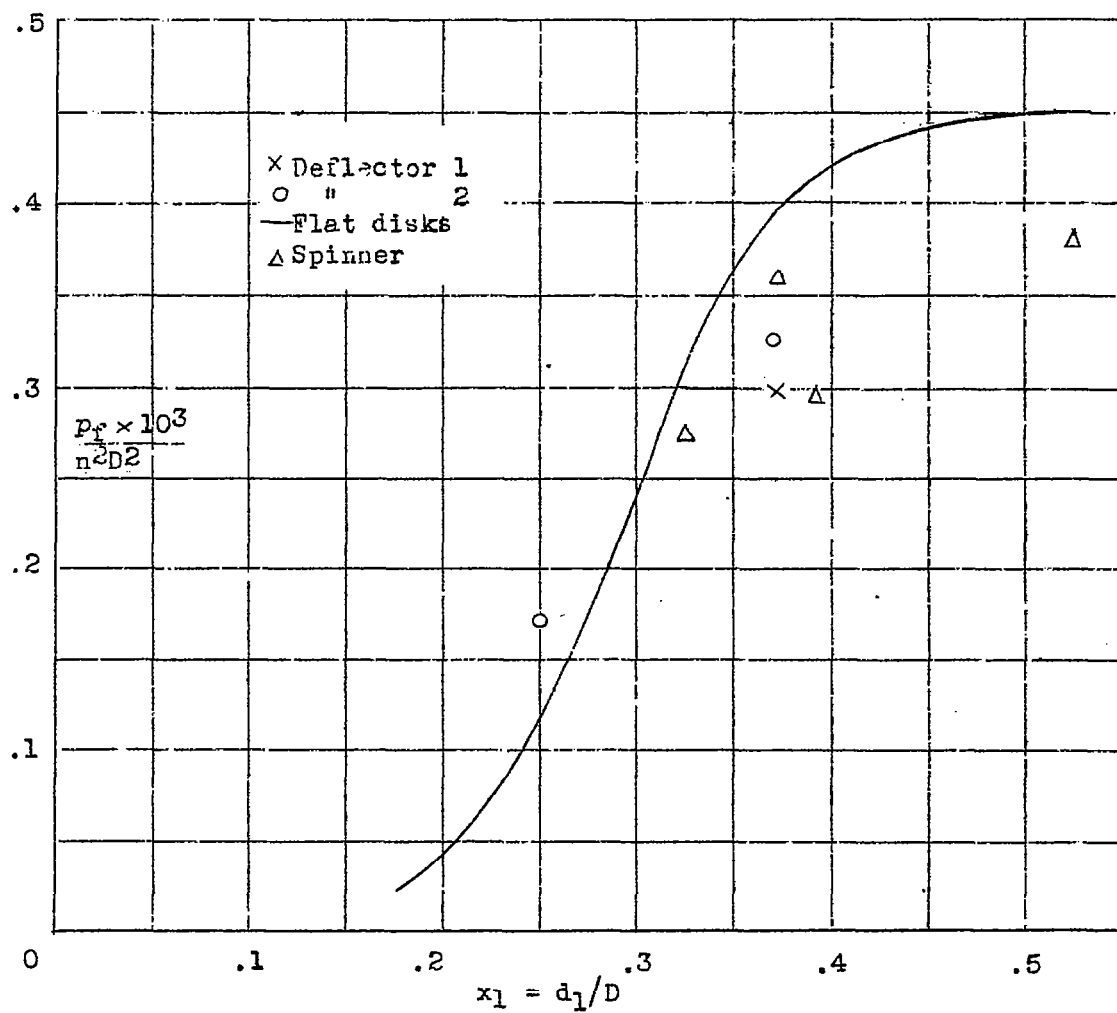


Figure 7.- Comparison of the effect of deflectors, flat disks and spinners on the average front pressure. Propeller C, blade angle  $15^\circ$  at 0.75 R,  $K = 0$ .



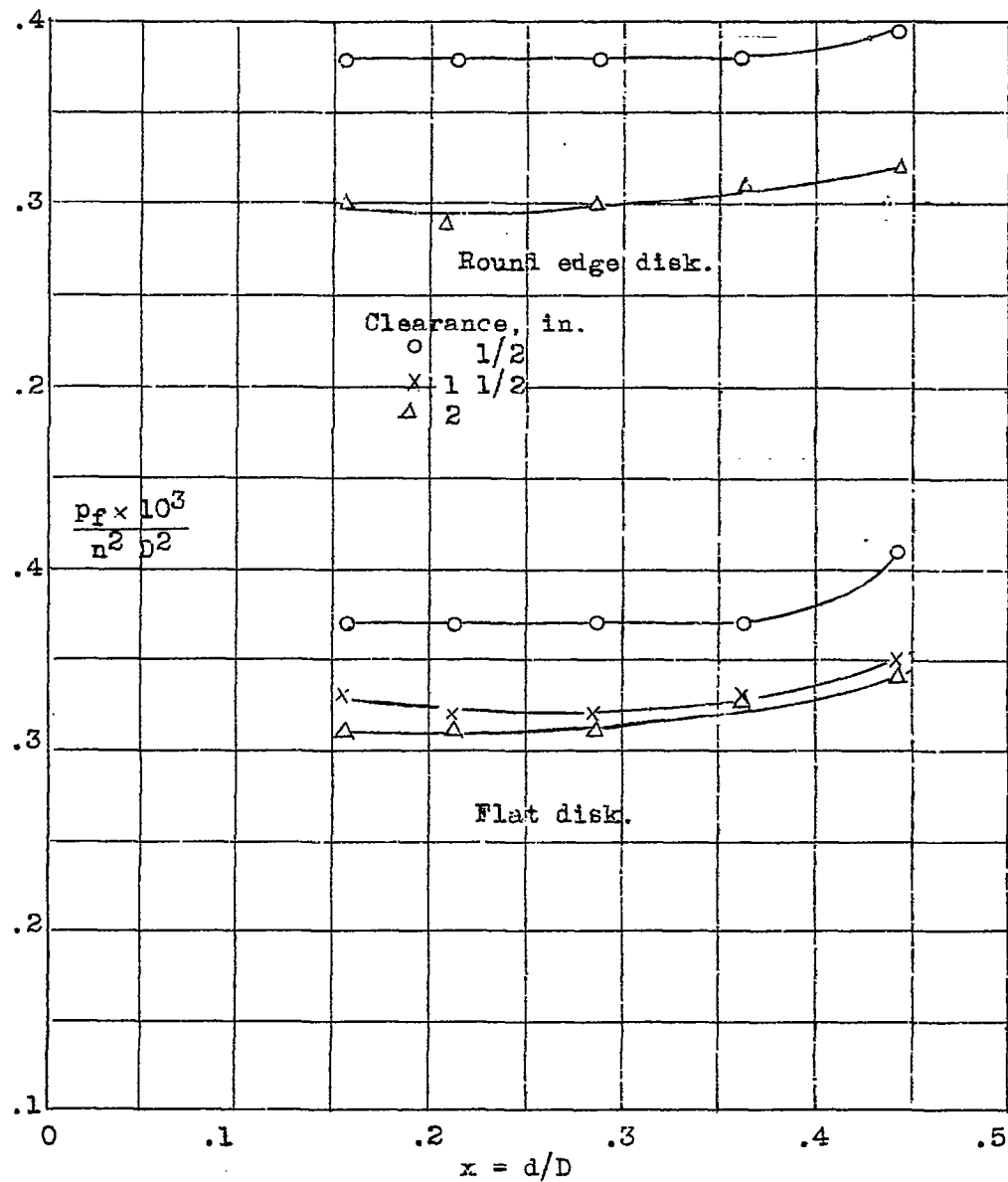


Figure 8.- Radial pressure distribution across the cowling as affected by the distance between the propeller and the cowling nose. Propeller C, blade angle  $15^\circ$  at  $0.75 R$ ,  $K = 0$ .

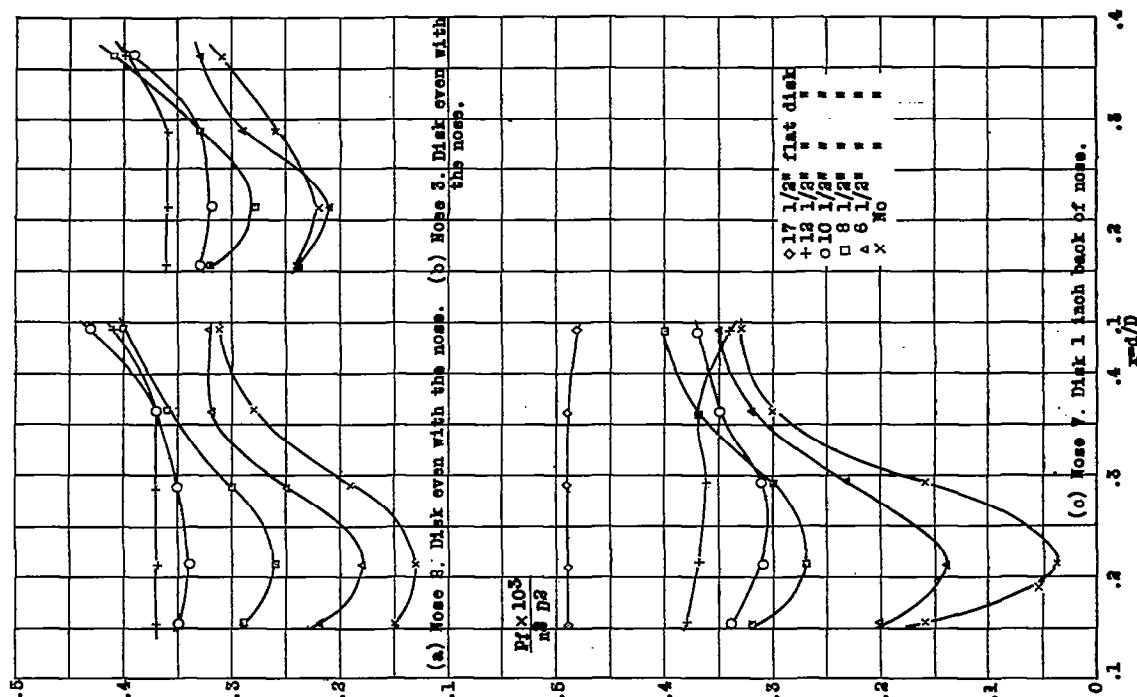


Figure 10.- Radial pressure distribution as affected by size of flat disk. Propeller C set 15° at 0.75 R; 1/2-inch propeller clearance;  $K = 0$ .

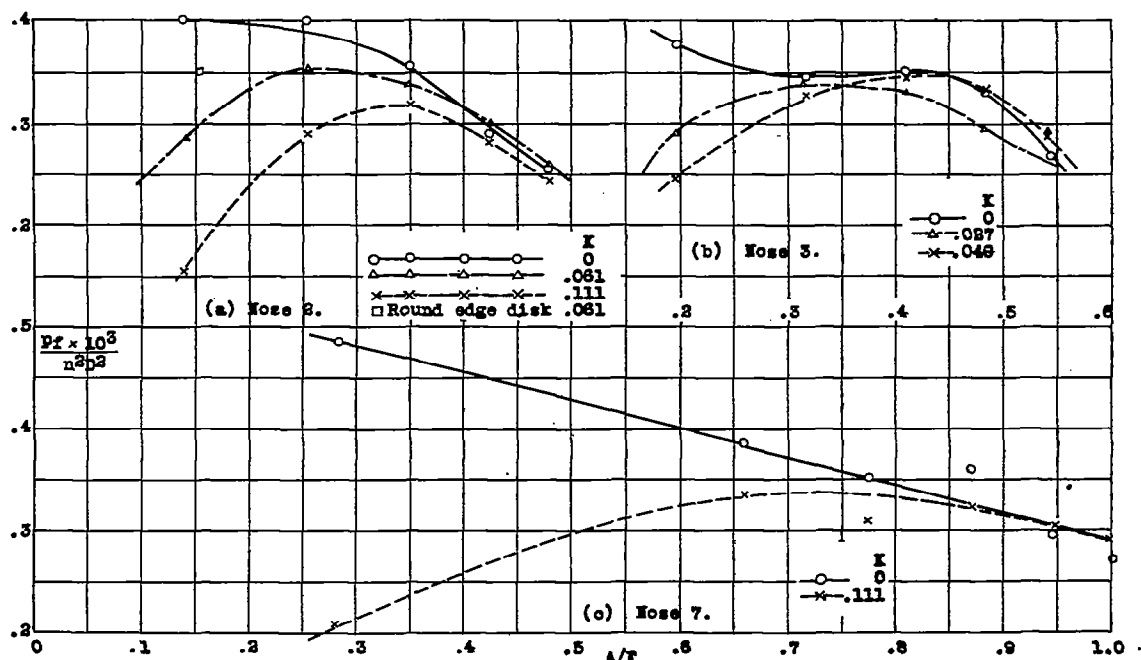


Figure 11.- Average front pressure obtained with various engine conductivities, plotted as a function of area of front opening, Propeller C; blade angle 15° at 0.75 R; 1/2-inch propeller clearance.